Supporting Information

Structural and Mechanistic Insights into KslB, a Bacterial Pictet-Spenglerase in Kitasetaline Biosynthesis

Wantae Kim[1,*], Ziyang Zheng[2,*], Kangsan Kim[3], Yu-Hsuan Lee[4], Hung-wen Liu[2,4,#] and Y. Jessie Zhang[3,#]

[1]McKetta Department of Chemical Engineering, University of Texas at Austin, Austin, Texas 78712, United States

[2]Department of Chemistry, University of Texas at Austin, Austin, Texas 78712, United States

[3]Department of Molecular Biosciences, University of Texas at Austin, Austin, Texas 78712, United States

[4]Division of Chemical Biology and Medicinal Chemistry, College of Pharmacy, University of Texas at Austin, Austin, Texas 78712, United States

[*]These authors contributed equally to this work.

[#]Correspondence should be addressed to: Hung-wen Liu (h.w.liu@mail.utexas.edu) and Y. Jessie Zhang (jzhang@cm.utexas.edu).

Table of Contents

Experimental Procedures

S1. Materials and instrumentation

Oligonucleotide primers were prepared by Integrated DNA Technologies (Coralville, IA). Kits for DNA gel extraction and spin minipreps are products of Qiagen (Valencia, CA). Enzymes and molecular weight standards used in the cloning experiments were obtained from New England Biolabs (Ipswich, MA). Q5® High-Fidelity DNA polymerase and restriction enzymes were acquired from New England Biolabs (Ipswich, MA). Reagents for sodium dodecyl sulfate polyacrylamide gel electrophoresis (SDS-PAGE) were purchased from Bio-Rad (Hercules, CA). YM-10 ultrafiltration membranes are products of Millipore (VWR, PA). DNA and protein concentrations were measured using a NanoDrop ND-1000 UV−vis instrument from Thermo Fisher Scientific. HPLC analysis was performed using an Agilent Technologies HPLC system equipped with a pump (G1311C), an auto sampler (G1329B), and an Agilent HPLC diode array detector (G1315D).

S2. Cloning, protein expression and purification of KslB

Two linear fragments were separately PCR-amplified from the wild-type kslB/pET28b(+) plasmid using one mutagenesis primer and one backbone primer shown in Table S1. These two fragments were ligated with HiFi DNA Assembly (NEB) to generate the corresponding plasmids. The sequences were confirmed by DNA sequencing. The expression and purification of KslB variants are the same as reported for the wild-type KslB[1]. The SDS-PAGE of purified enzymes are shown in Figure S1. To obtain highly purified KslB for crystallization, recombinant KslB proteins were further refined using size-exclusion fast protein liquid chromatography (SEC-FPLC) with a HiLoad Superdex 75 column (Cytiva) after dialysis against SEC buffer (20 mM Tris-HCl pH 7.5, 200 mM NaCl, 10 mM β-mercaptoethanol, and 1 mM L-Trp). The purified protein was then concentrated to 10 mg/mL using a Vivaspin 20 centrifugal concentrator (Sartorius), flash-frozen in liquid nitrogen, and stored at –80°C until crystallization.

S3. *In vitro* enzymatic assays

A solution of 1 mM L-tryptophan was incubated with 5 μM KslB or its variant, and 1 mM α-KG or 1 mM succinic semialdehyde (SSA) in 50 mM 4-(2-hydroxyethyl)-1-piperazineethanesulfonic acid (HEPES) buffer (pH 7.5) at room temperature in a volume of 50 μL for 16 h. The protein was removed using YM-10 centrifugal filtration. The resulting filtrate was analyzed by HPLC using Poroshell 120 EC-C18 column (2.7 μm, 4.6 × 100 mm) with Eclipse plus C18 guard column (1.8 μm, 2.1 × 5 mm) at a flow rate of 0.4 mL/min using 0.1% formic acid (FA) in H_2O (solvent A) and acetonitrile (solvent B) with the following gradient program unless otherwise specified: 0–15 min 5–95% B, 15–17 min 95% B, 17–18 min 95–5% B, 18–20 min 5% B. Elution of the compounds was monitored by setting the UV-detector at 276 nm.

S4. KslB protein crystallization

Purified KslB was concentrated to 10 mg/mL and directly used for sparse matrix screening to identify initial crystallization conditions. Rod-shaped crystals appeared after incubation at room temperature for three days. Crystallization conditions were further optimized using sitting-drop vapor diffusion, systematically varying pH and precipitant composition. Crystals suitable for X-ray diffraction were obtained in a solution containing 0.1 M bis-Tris (pH 5.5), 0.2 M sodium chloride (or magnesium chloride), and 15–20% (w/v) PEG 3350. For KslB-ligand complex crystallization, purified protein with 1mM L-Trp in buffer was incubated on ice for 3 hours with a final concentration of 5mM *N*-oxalylglycine, α-ketoglutaric acid, and succinic semialdehyde respectively. Crystal seeding was employed to promote co-crystal growth (Seed Bead ™ Kits, Hampton Research).

S5. X-ray data collection, and structure determination

Individual crystals were flash-frozen in liquid nitrogen after brief incubation with the reservoir solution supplemented with 30% (v/v) glycerol as a cryoprotectant. X-ray diffraction data were collected at the

Advanced Light Source (ALS, Berkeley, CA, USA) using beamlines 5.0.1, 5.0.3, and 8.2.2. X-ray diffraction data were processed with HKL2000[2]. The AlphaFold model[3] of KslB was used as a search model to determine the initial phase by molecular replacement. The refinement was conducted iteratively with Coot[4] and Phenix[5] packages to build the model. The quality of the refined models were evaluated by MolProbity[6]. The final statistics for data collection and structure determination are shown in Table S2.

S6. Differential scanning fluorimetry

The differential scanning fluorimetry (DSF) assay was conducted with KslB at a final concentration of 5 µM in a 96-well qPCR plate, with each sample set up in technical duplicates. 10× SYPRO Orange (10 µM, Molecular Probes) was added to each well, mixed, and measured using a qPCR instrument (LightCycler 480, Roche). Protein melting experiments were performed under continuous heating from 25°C to 95°C at a rate of +0.5 °C/min. The melting temperature (T_m) was determined by analyzing the first derivative of the fluorescence data, fitted using the Boltzmann equation.

S7. Docking with Autodock Vina

The initial 3D coordinates of the imine intermediate (**9**) were obtained by using SMILES string (O=C(O)CC/C(=[NH+]/[C@@H](Cc1c[nH]c2ccccc12)C(=O)O)C(=O)O) as an input for phenix elbow[7]. This ligand coordinate was docked into the binding pocket of apo KslB structure. Docking with Autodock Vina[8, 9] was repeated with different protein chains with different seeds and all docked poses were manually screened based on the known binding modes of L-Trp. The docked poses that best satisfy the mechanistic insight was used for generating publication quality figures. The calculated binding affinity scores are 7.831 kcal/mol (chain A), -7.716 kcal/mol (chain B), -7.120 kcal/mol (chain C), -7.643 kcal/mol (chain D), -7.389 kcal/mol (chain E), and -7.397 kcal/mol (chain F).

Supplementary Figures

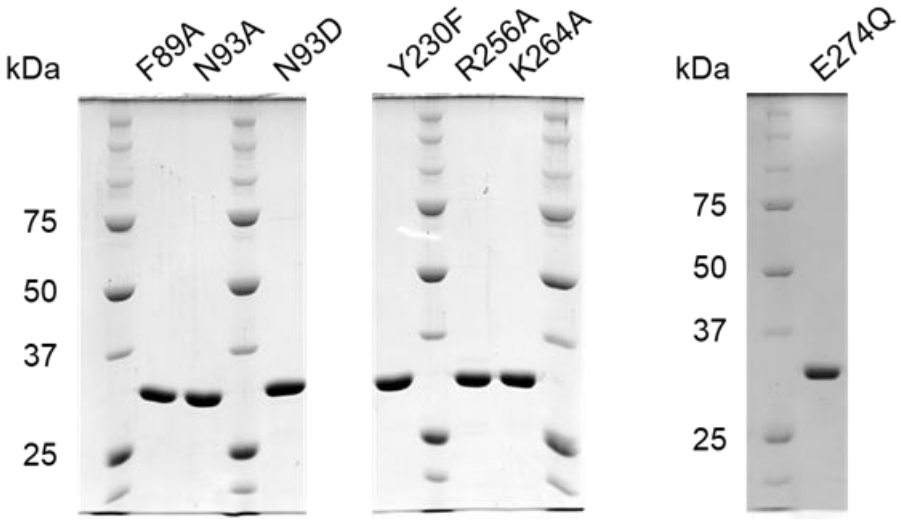

Figure S1. SDS-PAGE analysis of purified *N*-His_6-tagged KslB variants.

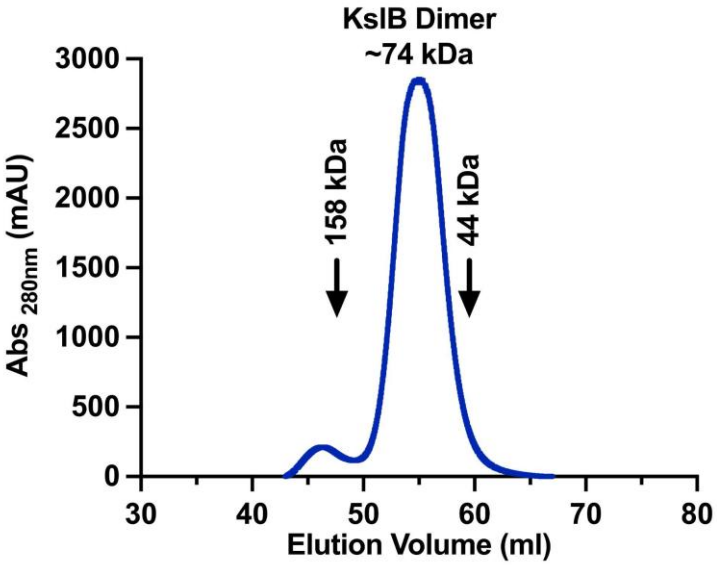

Figure S2. Size exclusion chromatography (SEC) profile of KslB. Recombinant KslB exists as a homodimer in solution (monomer: 36.9 kDa, dimer: 73.8 kDa).

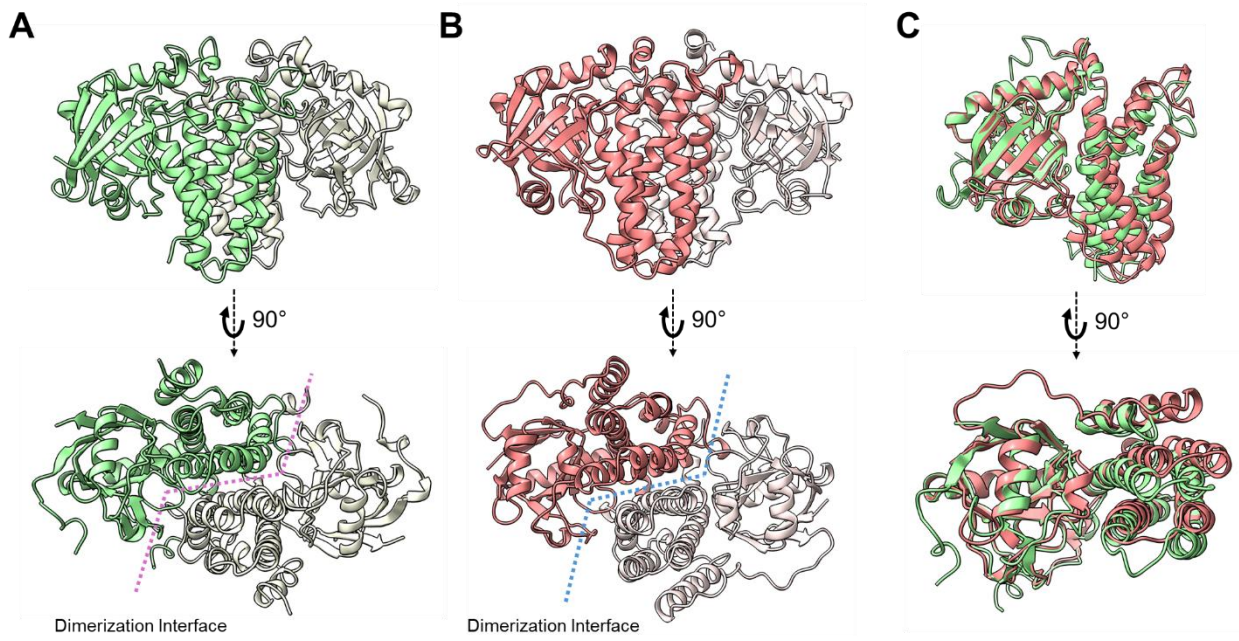

Figure S3. Structural comparison between KslB and McbB. (A) Overall homodimer structure of KslB. (B) Overall homodimer structure of McbB. (C) Superimposed structure of KslB (Green cartoon) and McbB (Red cartoon) monomers.

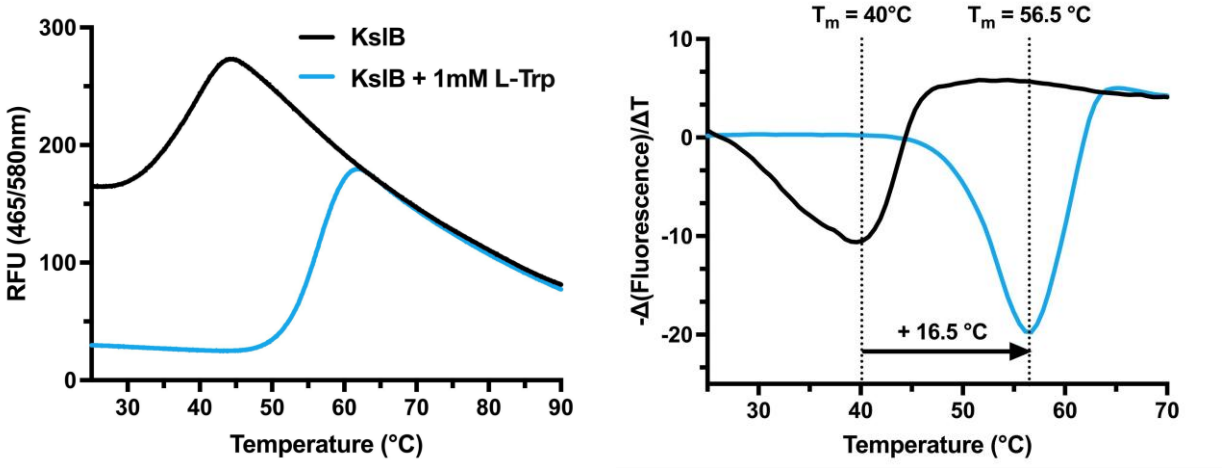

Figure S4. Stabilization effect of L-Trp binding on KslB thermal stability measured by protein melting temperature (T_m). Representative DSF melting curves for KslB with and without L-Trp. Raw fluorescence data (left) and its first derivative (right).

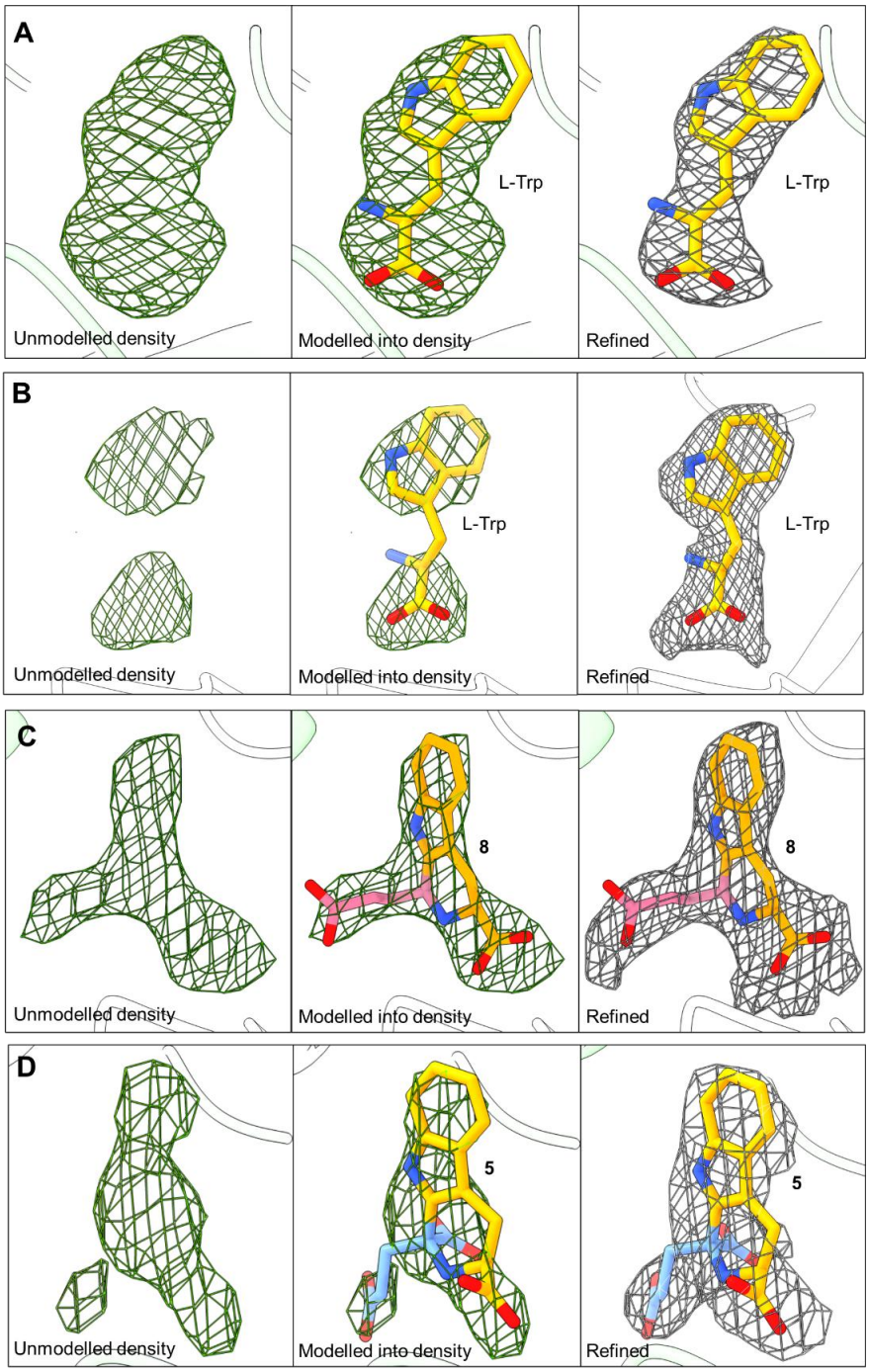

Figure S5. Electron density maps before and after modelling (A) L-Trp (B) L-Trp in a different conformation (C) 8 and (D) 5 into corresponding x-ray diffraction data. For each panel, (left) the F_o-F_c map (green mesh, contoured at 2.5σ) are calculated with no phase information. (middle) ligand was built and fitted on the map. (right) $2F_o$-F_c map (gray mesh, contoured at 1.0σ) are shown on top of the stick models.

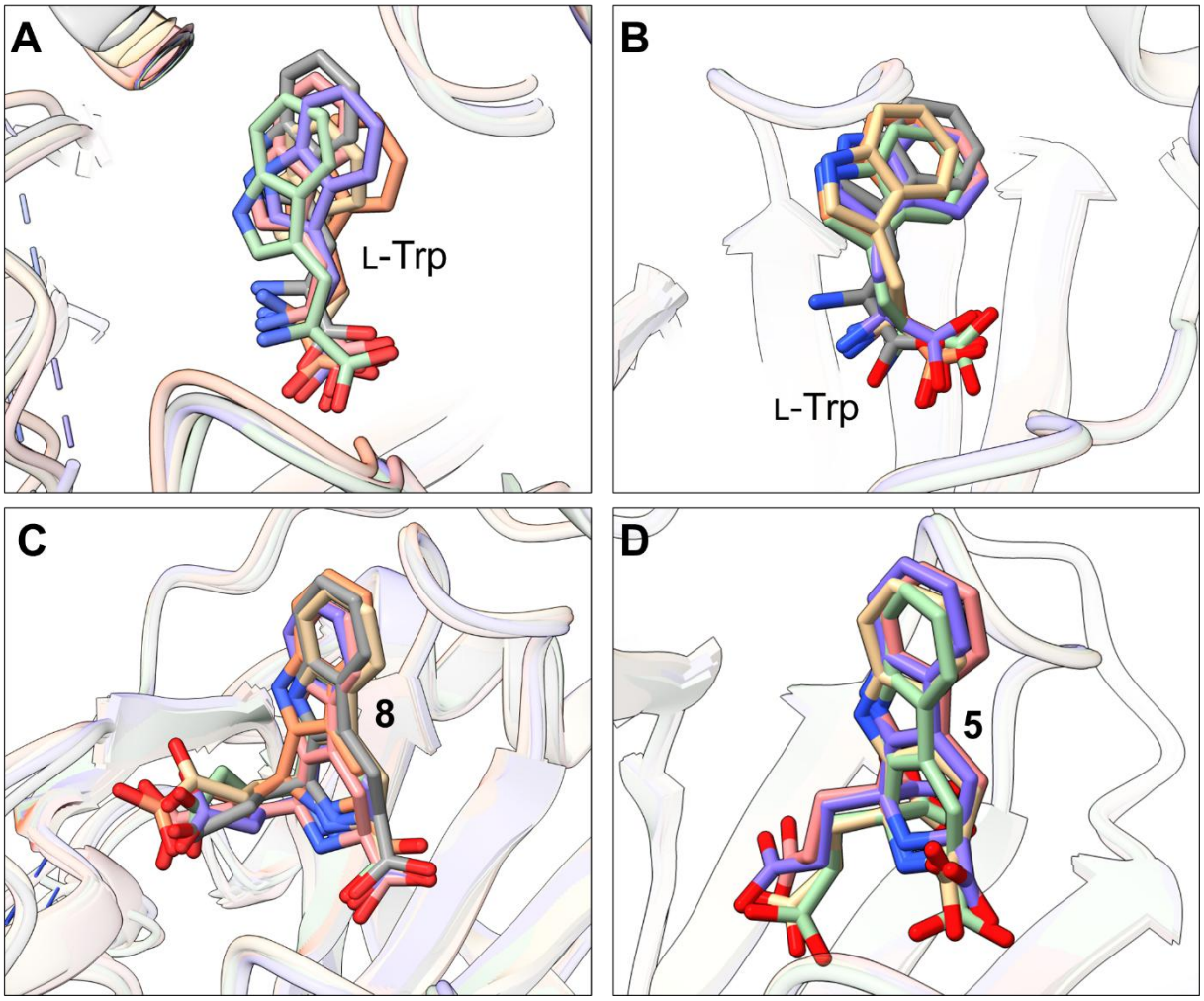

Figure S6. Superposed (A) L-Trp, (B) L-Trp in an alternative conformation (C) 8, and (D) 5 binding sites of six protein chains within a crystal asymmetric unit. For **5**, only chain A, B, C, and D are built with the ligand. Color scheme : Chain A – Purple, Chain B – Pink, Chain C – Green, Chain D – Beige, Chain E – Orange, and Chain F – Gray.

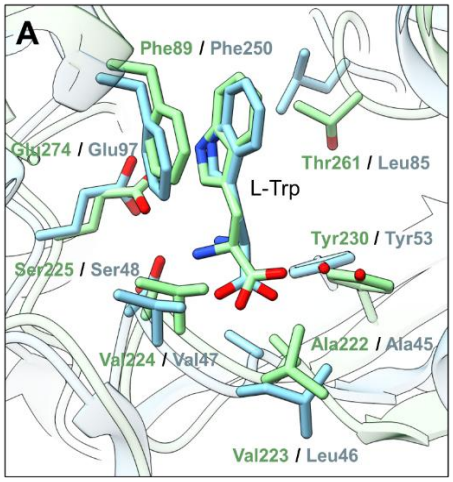

B

```
McbB_Nterminus   4    IEIEWVQPGITVTADLSWERNPELAELLWTGLLPYNSLQNHALVSGNHLVHLIADPRLVY  63
                      + + W   G+ V A++  + NP+LA  +   L P+  LQ+HA+VSG  +V     P +
KslB_Cterminus   182  VRLTWQPLGVQVDAEIYADLNPQLATDVLKAL-PFTVLQDHAVVSGESMLAWA--PLVSV  238

McbB_Nterminus   64   TEARYKEDRTKSPDGTVFLSQL--QHLAVKYGPLTHYLPAAPVGSVVPEDIDALREAGRA  121
                        +E    +P G +  SQ     + V+YGP T  L +  +G VV    D L E G+A
KslB_Cterminus   239  APTPVRERICDAPVGRLRFSQATGNKVIVQYGPTTETLSSPVLGKVVDSHADRLAEVGKA  298

McbB_Nterminus   122  CWKAAWETKQPIEVRVRR  139
                       W++ + +K+P+ + V R
KslB_Cterminus   299  VWESTFSSKEPVWLTVER  316

McbB_Cterminus   179  PAEIVDMHQGRIASRAGSYDQYFSTLVFLNGEVRPLGYCALNGLLKICRTTDLTLNDLKR  238
                      P EI  +  G +    GSY QYF+   F N  VR      L  L ++     +++ +L
KslB_Nterminus   19   PPEIRRIRTGTVPDLPGSYGQYFTAWDFSNSIVRDYA-MNLYQLTRLATDESVSVENLLT  77

McbB_Cterminus   239  ITPTFIKTPAEFLGYTGLDTLWRFTQQVLTLLPDVETREQYFALVNALALYANMLNTWNL  298
                      +  T     +  FLGY G   L  + Q+V       E+R +    +     Y N L  W+
KslB_Nterminus   78   VFRTLDPIYSTFLGYNGFPVLAEYAQRVGQ---PAESRAELLDRLTTFTEYVNRLTAWSH  134

McbB_Cterminus   299  HFFPWQHGTD-YRY  311
                      H+FPW  G + YRY
KslB_Nterminus   135  HYFPWDLGGERYRY  148
```

Figure S7. Active site residues that are conserved between McbB and KslB. (A) Superposed L-Trp binding sites of KslB (Green) and McbB (Blue, PDB code 3X27). (B) Sequence alignment of McbB and KslB. Conserved residues that interact with L-Trp are highlighted in green.

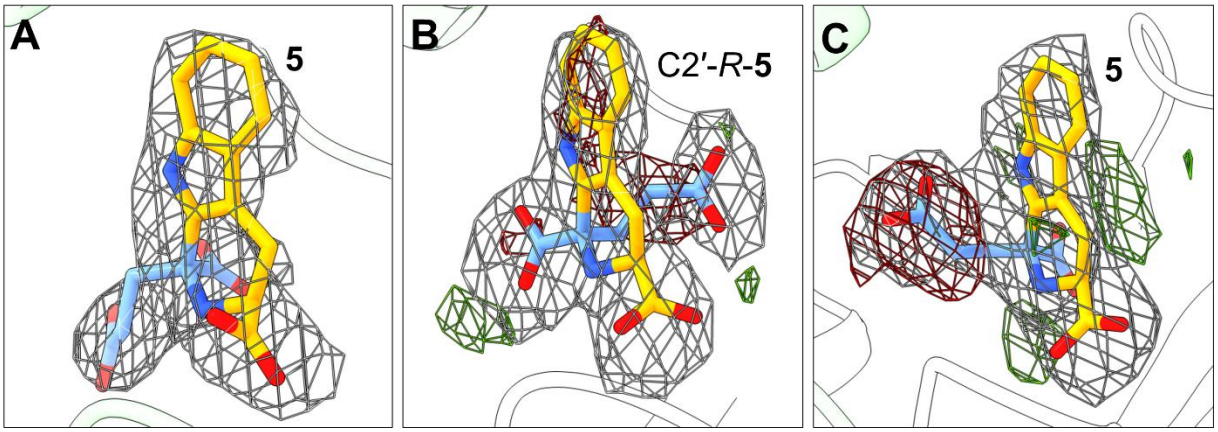

Figure S8. Electron density map after fitting (A) *S*-configured KslB reaction product (5), (B) Hypothetical *R*-configured product (C2′-*R*-5), and (C) Binding pose of 5 from the soaked crystal structure[10] and KslB·8 structure into KslB·5 co-crystal diffraction data. $2F_o$-F_c map (gray mesh, contoured at 1.0σ) and F_o-F_c map (green and maroon mesh, contoured at +3.0σ and -3.0σ respectively) are superposed on top of stick models. Atoms from KslB catalyzed Pictet-Spenglerase substrates, L-Trp and α-KG, are respectively colored yellow and blue.

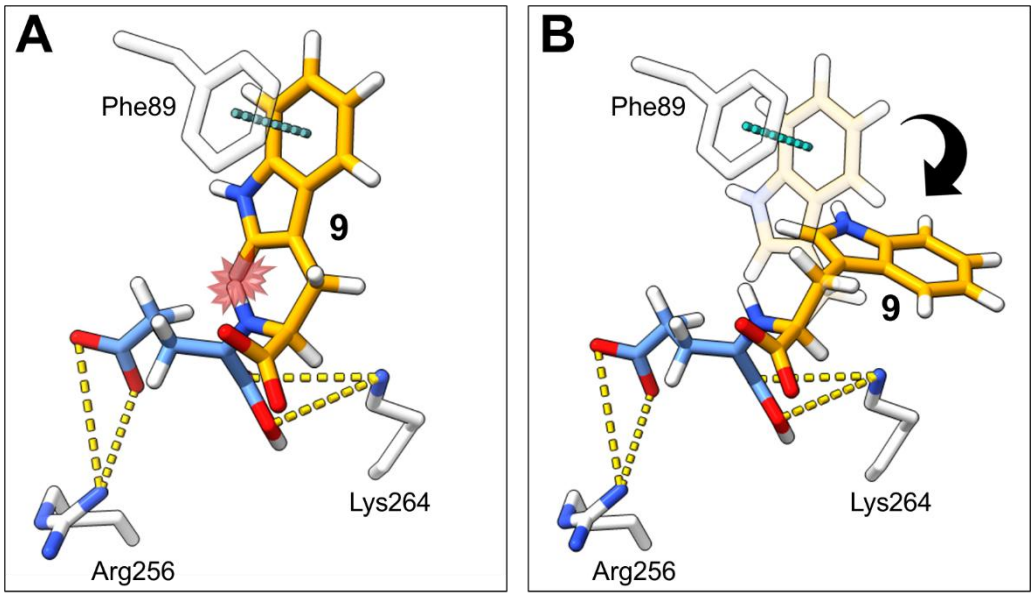

Figure S9. Comparison of binding poses of 9 when adopting (A) the known conformation of L-Trp and (B) alternative binding mode of L-Trp. Hydrogen bonding interactions and π-π stacking interactions are shown as yellow and green dashed lines respectively.

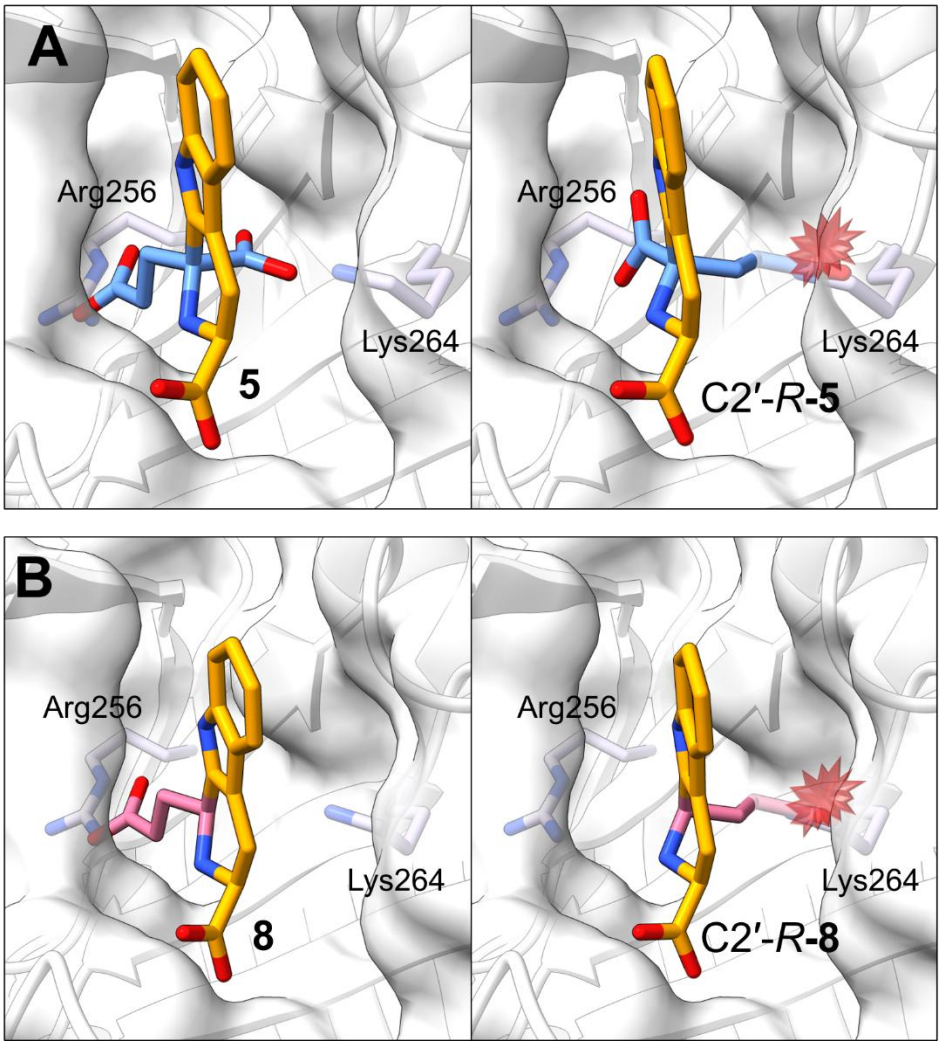

Figure S10. Structural analysis on stereoselectivity of KslB during formation of 5 or 8. (A) Experimentally determined binding pose of **5** (C2′-*S*, left) and computationally modelled diastereomer (C2′-*R*, right) within the active site surface of KslB. (B) Computationally modelled binding pose of **8** (C2′-*S*, left) and diastereomer (C2′-*R*, right) within the active site of KslB. Atoms from L-Trp, α-KG, and **7** are colored yellow, blue, and pink respectively. Possible steric clashes are shown as red explosion icons.

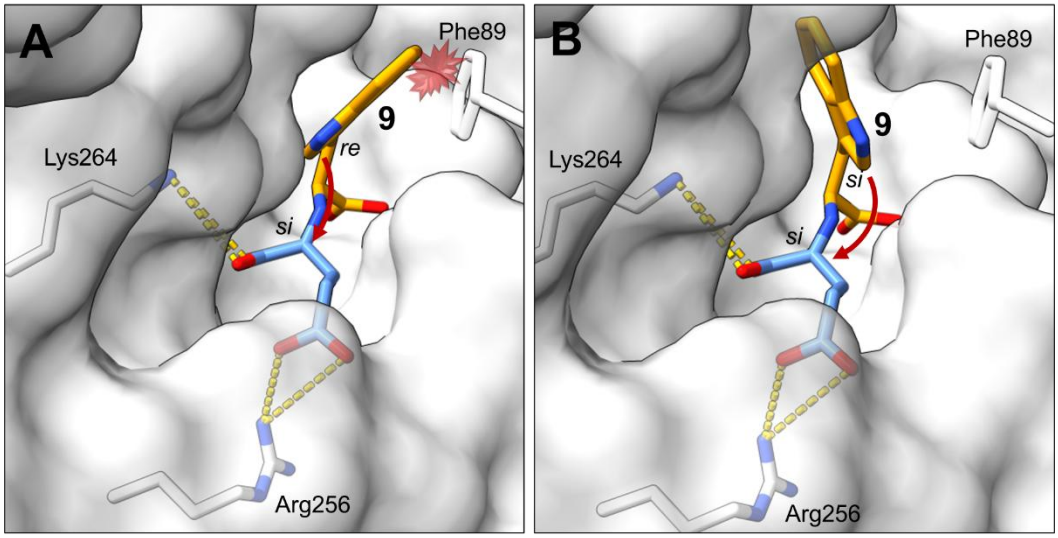

Figure S11. The (A) *re* and (B) *si* face nucleophilic attack from indole ring of 9.

Supplementary Tables

Table S1. Primers used in the mutagenesis of KslB.

Primer	**Sequence (5′ → 3′)**
F89A-fwd	GATCTACAGCACC**gc**CCTCGGCTACAACGGGTT
F89A-rev	GTAGCCGAGG**gc**GGTGCTGTAGATCGGGT
N93A-fwd	TTCCTCGGCTAC**gc**CGGGTTCCCGGTCCT
N93A-rev	ACCGGGAACCCG**gc**GTAGCCGAGGAAGGT
N93D-fwd	TTCCTCGGCTAC**g**ACGGGTTCCCGGTCCT
N93D-rev	ACCGGGAACCCGT**c**GTAGCCGAGGAAGGTG
Y230F-fwd	GAGTCCATGT**t**CGCCTGGGCCCCCCTGGTGA
Y230F-rev	GGCCCAGGCG**a**ACATGGACTCGCCGCT
R256A-fwd	GGTCGGCCGGCT**tgc**GTTCAGCCAGGCGACC
R256A-rev	CTGGCTGAAC**gca**AGCCGGCCGACCGG
K264A-fwd	GCGACCGGCAAC**gc**GGTCATCGTCCAGTA
K264A-rev	TGGACGATGACC**gc**GTTGCCGGTCGCCTGGCT
E274Q-fwd	GGGCCGACCACG**c**AGACGCTCAGCAGTCC
E274Q-rev	TGCTGAGCGTCT**g**CGTGGTCGGCCCGTACT
backbone-fwd	CACAGATGTCTGCCTGTTCATCCGCGTCCAGCTCGTTGAG
backbone-rev	CTCAACGAGCTGGACGCGGATGAACAGGCAGACATCTGTG

Table S2. Crystallographic data collection and refinement statistics.

	KslB Apoenzyme	KslB · L-Trp	KslB · L-Trp (*N*-oxalylglycine)	KslB · 5 (α-ketoglutaric acid)	KslB · 8 (succinic semialdehyde)
PDB entry	**9NS6**	**9NSC**	**9NSS**	**9NST**	**9NSU**
Data Collection					
Space group	P 3_2	P 3_2	P 3_2	P 3_2	P 3_2
Cell Dimension					
Resolution (Å)	47.80 - 2.95 (3.00 – 2.95) *	47.27-3.10 (3.15 – 3.10)	47.60 – 2.68 (2.75 – 2.68)	47.78 – 3.30 (3.39 – 3.30)	47.04 - 2.87 (2.94 – 2.87)
Unit cell: a, b, c (Å)	95.59, 95.59, 193.40	94.53, 94.53, 193.10	95.20, 95.20, 193.49	95.57, 95.57,193.65	94.083, 94.083, 193.415
Unit cell: α, β, γ (°)	90, 90, 120	90, 90, 120	90, 90, 120	90, 90, 120	90, 90, 120
R_{sym} / R_{pim}	0.120 (0.613) / 0.092 (0.466)	0.226 (0.621) / 0.143 (0.454)	0.171 (0.744) / 0.084 (0.455)	0.241 (0.777) / 0.170 (0.597)	0.142 (1.081) / 0.069 (0.589)
$CC_{1/2}$[Y]	0.975 (0.540)	0.924 (0.500)	0.981 (0.571)	0.942 (0.346)	0.997 (0.538)
I / σ	5.2 (1.0)	3.5 (0.9)	6.1 (0.8)	3.0 (0.9)	7.5 (0.6)
Completeness (%)	97.2 (98.1)	99.9 (99.0)	98.8 (86.1)	98.9 (97.5)	99.3 (87.6)
Redundancy	2.6 (2.6)	3.4 (2.8)	5.0 (3.1)	2.9 (2.5)	5.1 (3.3)
Refinement					
Resolution (Å)	47.80 - 2.95 (3.00 – 2.95)	47.27 - 3.10 (3.18 – 3.10)	46.60 – 2.67 (2.75 – 2.68)	47.78 – 3.30 (3.39 – 3.30)	47.04 – 2.87 (2.94 – 2.87)
No. reflections	40045 (2813)	34323 (2387)	53703 (3292)	28836 (1932)	42184 (2612)
R_{work}	0.2068 (0.2561)	0.1765 (0.2222)	0.2032 (0.2568)	0.1943 (0.2507)	0.2238 (0.2804)
R_{free}[±]	0.2478 (0.2910)	0.2342 (0.3265)	0.2230 (0.2755)	0.2133 (0.2599)	0.2613 (0.2865)
No. Atoms					
Protein	13615	13934	13834	14123	13241
Ligand	-	90	90	96	126
B- factors (Å²)					
Protein	46.8	42.1	43.3	55.2	66.4
Ligand	-	55.5	39.9	55.6	67.4
R.m.s deviations					
Bond lengths (Å)	0.012	0.012	0.011	0.002	0.012
Bond angles (°)	1.27	1.46	1.39	0.51	1.55
Ramachandran plot					
Favored (%)	94.81	95.39	94.35	98.12	95.79
Allowed (%)	5.19	4.61	5.65	1.88	4.21
Outliers (%)	0.00	0.00	0.00	0.0	0.00
Molprobity score^	2.59 (92nd percentile)	2.62 (94th percentile)	2.67 (77th percentile)	1.38 (100th percentile)	2.96 (72nd percentile)

*Values for the corresponding parameters in the outermost shell in parenthesis. [Y]CC1/2 is the Pearson correlation coefficient for a random half of the data, the two numbers represent the lowest and highest resolution shell, respectively. [±]R_{free} is the R_{work} calculated for about 10% of the reflections randomly selected and omitted from refinement. ^MolProbity score is calculated by combining clashscore with rotamer and Ramachandran percentage and scaled based on X-ray resolution. The percentage is calculated with 100th percentile as the best and 0th percentile as the worst among structures of comparable resolution.

References

1. Z. Zheng, H. Choi and H.-w. Liu, *Journal of the American Chemical Society*, 2024, **146**, 28553-28560.
2. Z. Otwinowski and W. Minor, in *Methods in Enzymology*, Academic Press, 1997, vol. 276, pp. 307-326.
3. J. Jumper, R. Evans, A. Pritzel, T. Green, M. Figurnov, O. Ronneberger, K. Tunyasuvunakool, R. Bates, A. Žídek, A. Potapenko, A. Bridgland, C. Meyer, S. A. A. Kohl, A. J. Ballard, A. Cowie, B. Romera-Paredes, S. Nikolov, R. Jain, J. Adler, T. Back, S. Petersen, D. Reiman, E. Clancy, M. Zielinski, M. Steinegger, M. Pacholska, T. Berghammer, S. Bodenstein, D. Silver, O. Vinyals, A. W. Senior, K. Kavukcuoglu, P. Kohli and D. Hassabis, *Nature*, 2021, **596**, 583-589.
4. P. Emsley and K. Cowtan, *Acta Crystallogr. D Biol. Crystallogr.*, 2004, **60**, 2126–2132.
5. D. Liebschner, P. V. Afonine, M. L. Baker, G. Bunkoczi, V. B. Chen, T. I. Croll, B. Hintze, L.-W. Hung, S. Jain, A. J. McCoy, N. W. Moriarty, R. D. Oeffner, B. K. Poon, M. G. Prisant, R. J. Read, J. S. Richardson, D. C. Richardson, M. D. Sammito, O. V. Sobolev, D. H. Stockwell, T. C. Terwilliger, A. G. Urzhumtsev, L. L. Videau, C. J. Williams and P. D. Adams, *Acta Crystallographica Section D*, 2019, **75**, 861-877.
6. V. B. Chen, W. B. Arendall, 3rd, J. J. Headd, D. A. Keedy, R. M. Immormino, G. J. Kapral, L. W. Murray, J. S. Richardson and D. C. Richardson, *Acta Crystallogr D Biol Crystallogr*, 2010, **66**, 12-21.
7. N. W. Moriarty, R. W. Grosse-Kunstleve and P. D. Adams, *Acta Crystallographica Section D Biological Crystallography*, 2009, **65**, 1074-1080.
8. J. Eberhardt, D. Santos-Martins, A. F. Tillack and S. Forli, *Journal of Chemical Information and Modeling*, 2021, **61**, 3891-3898.
9. O. Trott and A. J. Olson, *Journal of Computational Chemistry*, 2010, **31**, 455-461.
10. R. Jiang, N. Wasfy, T. Mori, M. Hoang, I. Abe and H. Renata, *ChemRxiv*, 2025, DOI: 10.26434/chemrxiv-2025-fvct3.